



Two-dimensional physical-based inversion of confined and unconfined aquifers under unknown boundary conditions



Jianning Jiao*, Ye Zhang*

Department of Geology and Geophysics, University of Wyoming, Laramie, WY, United States

ARTICLE INFO

Article history:

Received 1 March 2013

Received in revised form 23 July 2013

Accepted 24 October 2013

Available online 15 November 2013

Keywords:

Aquifer calibration

Inverse method

Hydraulic conductivity

Recharge rate

Structure error

Equivalent parameter

ABSTRACT

An inverse method is developed to simultaneously estimate multiple hydraulic conductivities, source/sink strengths, and boundary conditions, for two-dimensional confined and unconfined aquifers under non-pumping or pumping conditions. The method incorporates noisy observed data (hydraulic heads, groundwater fluxes, or well rates) at measurement locations. With a set of hybrid formulations, given sufficient measurement data, the method yields well-posed systems of equations that can be solved efficiently via nonlinear optimization. The solution is stable when measurement errors are increased. The method is successfully tested on problems with regular and irregular geometries, different heterogeneity patterns and variances (maximum K_{\max}/K_{\min} tested is 10,000), and error magnitudes. Under non-pumping conditions, when error-free observed data are used, the estimated conductivities and recharge rates are accurate within 8% of the true values. When data contain increasing errors, the estimated parameters become less accurate, as expected. For problems where the underlying parameter variation is unknown, equivalent conductivities and average recharge rates can be estimated. Under pumping (and/or injection) conditions, a hybrid formulation is developed to address these local source/sink effects, while different types of boundary conditions can also exert significant influences on drawdowns. Local grid refinement near wells is not needed to obtain accurate results, thus inversion is successful with coarse inverse grids, leading to high computation efficiency. Furthermore, flux measurements are not needed for the inversion to succeed; data requirement of the method is thus not much different from that of interpreting classic well tests. Finally, inversion accuracy is not sensitive to the degree of nonlinearity of the flow equations. Performance of the inverse method for confined and unconfined aquifer problems is similar in terms of the accuracy of the estimated parameters, the recovered head fields, and the solver speed.

© 2013 Elsevier Ltd. All rights reserved.

1. Introduction

Model calibration is a standard tool for developing predictive hydrogeologic models. In both confined and unconfined aquifers, groundwater flow is not only influenced by the intrinsic hydraulic parameters of the aquifer, e.g., hydraulic conductivity (K), transmissibility (T), and storage coefficients, but also these source/sink effects due to areal recharge (or inter-formational leakage), evapotranspiration, and well operations. For a variety of scientific and management purposes, there exists a need to estimate not only the hydraulic parameters of the aquifers, but also the parameters that characterize these source/sink strengths. However, the simultaneous estimation of K (or T) and source/sink rates suffers a well-known issue of parameter identifiability. For example, if a homogeneous unconfined aquifer is receiving uniform recharge, the flow equation becomes: $\nabla^2(h^2) = -2N/K$, where ∇^2 is the Laplace operator and N is the recharge rate. Clearly, as long as the ratio of the

recharge rate versus conductivity remains the same, infinite combinations of these two parameters can yield identical hydraulic head distribution in the aquifer. In this case, fitting or inverting only the hydraulic head data cannot lead to the unique estimations of these two parameters. This is a limitation that cannot be overcome with any inverse methods. In this study, groundwater fluxes that are sampled in the subsurface under non-pumping conditions or well rates that are sampled at the surface under pumping (or injection) conditions are used to supplement the hydraulic head measurements in developing a new steady-state inverse method for both confined and unconfined aquifers. Based on these measurements, the method is able to simultaneously estimate hydraulic conductivities and recharge rates for aquifers where both parameters are also spatially inhomogeneous. In the following sections, a brief review of the existing techniques is provided, highlighting the need and motivation for developing the new inverse method.

A variety of techniques exist for estimating aquifer conductivities and recharge rates. On the one hand, traditional aquifer test methods develop type curves based on the assumption that aquifer

* Corresponding authors. Tel.: +1 3077669895.

E-mail addresses: jjiao1@uwyo.edu (J. Jiao), yzhang9@uwyo.edu (Y. Zhang).

conductivity is homogeneous or aquifer exhibits simple layering [1], although conductivity estimated with such assumptions can exhibit “scale effect” due to aquifer heterogeneity [2–4]. Other techniques employ slug tests, borehole flowmeters, and geophysical measurements to estimate the conductivities of small aquifer volumes near wellbores [5–8]. Methods have also been developed that combine geostatistics with the inverse theory to directly infer heterogeneous aquifer conductivity while quantifying its estimation uncertainty [13–15]. In most studies, however, source/sink effects such as the recharge rates were either not accounted for, assumed to be known (e.g., negligible recharge is a common assumption), or were eliminated using specialized formulations. On the other hand, extensive investigations have been carried out to estimate aquifer recharge, usually for unconfined systems [16]: some are based on water or chemical mass balances [17–21], others infer the recharge rates from physical-based, vadose-zone or rainfall-runoff models [22–24], while still others use model calibration and the inverse theory to infer recharge as one or more unknown parameters [25]. With the exception of model calibration, which can be used to simultaneously estimate hydraulic conductivities along with the recharge rates, many methods assume aquifer conductivity to be known, homogeneous, or piecewise homogeneous. For confined aquifers, recharge typically occurs as leakage, for which inverse methods are frequently used to infer the rates [26].

To estimate both conductivity and the recharge rate, many inverse methods are developed based on minimizing an objective function, which is typically defined as a form of mismatch between the measurement data and the corresponding model simulated values. During inversion, parameters are updated iteratively using a forward model, which requires the specification of the model boundary conditions (BC). However, in real aquifers, BC are typically unknown and assumptions of model BC may not reflect the actual subsurface conditions. To address this, Irsa and Zhang [9] developed a steady-state inverse method for confined aquifers by adopting a set of approximating functions for hydraulic heads and groundwater fluxes. The method, which did not rely on objective functions, can simultaneously estimate a single K , flow fields, and BC. However, source/sink effects (e.g., recharge, well operation) could not be accommodated, while the approximating functions employ polynomials without being attributed any physical meanings. To add source/sink, [27] extended this method by superposing analytical flow solutions to generate the approximating functions. Using nonlinear optimization, multiple conductivities (K s) and multiple recharge rates (N s) can be simultaneously estimated. Using observed heads and as few as a single pumping rate, the method was successfully tested on one-dimensional (1D) unconfined aquifer problems that are subject to various source/sink effects. Interestingly, for problems where the underlying parameter variabilities are unknown (e.g., the aquifer is assumed homogeneous with a constant recharge), equivalent conductivities and average recharge rates can be obtained. The method thus handles model “structure errors”, whereas the inverse parameterization simplifies or complexifies the true parameter fields. However, only 1D flows in simple geometries were tested, ability of this physical-based approach for solving realistic problems remains unknown. In particular, for problems with a pumping well, local grid refinement was needed to obtain accurate inverse solutions.

This paper extends and enhances the earlier studies by inverting two-dimensional aquifer problems with realistic source/sink effects, for both confined and unconfined aquifers with heterogeneous conductivity and recharge rates. By developing a set of hybrid approximating functions, an improved unified theory is presented, which addresses both non-pumping and pumping conditions. The problems explored in [9] under non-pumping conditions (i.e., subsurface groundwater fluxes must be sampled) and

in [27] for 1D flows under more general conditions are shown to be subsets or special cases of the unified theory. In the new formulation, well test solutions are implemented locally and inversion can be successfully carried out using a coarse grid. Local grid refinement (LGR) at the wells is not needed. This new formulation, which was not explored in the earlier studies, results in significant computational savings as the inversion system of equations remains small. Although using well tests to infer aquifer parameters has been investigated extensively in the literature for both homogeneous and heterogeneous media [28–35], areal source/sink effects are typically ignored and the aquifer boundaries must be placed far away from the well (alternatively, a suitably small aquifer K or well pumping rate was assumed). Therefore, with these methods, neither areal source/sink nor aquifer BC can influence pumping and the associated drawdowns. In the new formulation, for both confined and unconfined aquifers, BC can significantly affect drawdowns at the wells, e.g., a barrier wall placed close to a well resulting in increased drawdown compared to that of an infinite-BC solution. In addition, drawdowns can be simultaneously impacted by the BC and areal recharge, which does not affect the accuracy of parameter (and BC) estimation. The method can therefore address realistic problems where pumping (and/or injection) can be influenced by areal source/sink and nearby boundary characteristics.

The goals of this study are threefold: (1) We investigate the new physical-based approach (i.e., hybrid formulation) for inverting flows in confined and unconfined aquifers under both non-pumping and pumping conditions. (2) For problems where the underlying heterogeneities are unknown, we investigate whether equivalent conductivities and average recharge rates can be found. That is, at hydrogeological sites where highly detailed measurements are unattainable, can inverse methods provide estimates of large scale aquifer parameters that can represent the effects of unresolved small-scale variations? As demonstrated in a suite of upscaling studies [11,12], simplified hydrofacies models with equivalent parameters can capture certain bulk flow and conservative tracer transport behaviors without resolving all the detailed heterogeneity. (3) Comparing the performance of the inverse method between confined and unconfined flow problems, is the inversion accuracy affected by the degree of nonlinearity in the flow equation?

A fundamental contribution of our series of studies is to prove, via the new inverse method, that boundary condition information is not needed for estimating aquifer parameters, i.e., both the conductivities and the recharge rates. With the objective-function-based inversion techniques, hydraulic head and flux BC must be specified along the entire model boundary, because these methods require the repeated simulations of a forward model in order to minimize the objective function. For example, the often-adopted no-flux BC is in effect specifying a zero flux across the Neumann-type boundaries. One issue with these techniques lies in the fact that BC are typically unknown in real aquifers, and if a wrong set of BC is assumed, parameters estimated using objective functions are likely non-unique. As demonstrated in [9], two different sets of BC can give rise to two different flow fields both of which can perfectly fit the same observation data (3 heads and 1 flow rate), yielding a zero objective function. Although BC can be calibrated to evaluate its impact on parameter estimation, such an approach is likely inefficient. As demonstrated in [9], infinite combinations of parameters and BCs can fit the same observed data and non-uniqueness in calibrating the model parameters and model BC can only be eliminated at the limit where the observed data are sampled everywhere. These issues motivated our studies where we have demonstrated, via the new inverse method, that groundwater fluxes or well rates that are sampled anywhere in the solution domain can effectively replace the need for specifying the

model BC. Moreover, another issue with the objective-function based techniques is computation efficiency. For example, using global optimization (i.e., genetic algorithm, neural net, and others), thousands or more boundary value problems (BVPs) must be solved in the forward mode to minimize the objective function (and if BC are also calibrated, more BVPs must be solved). In our method, given appropriate measurement data, both parameters and unknown model BC can be simultaneously estimated without using objective functions. It is computationally efficient because the inversion involves a single step of equation assemblage – repeated solutions of the BVPs are not needed (an exception is when the inverse method is combined with geostatistics, whereas many parameter realizations are inverted to account for uncertainty in the static data [36]).

In the remainder of this article, the groundwater flow equations and the unified inverse theory implementing a hybrid formulation are introduced first, followed by results testing the theory for a variety of confined and unconfined aquifer problems. In each test problem, synthetic forward models are used to generate the true observation data under a set of true model BC. These data are provided to inversion to estimate model parameters and model BC, which are then compared to those of the forward models. The stability of the inverse solution is tested against increasing measurement errors. The issue related to model “structure errors” is also explored by estimating equivalent or average parameters when the parameter variability is unknown to inversion.

2. Theory

This study focuses on the inversion of a single confined or unconfined aquifer. In this section, mathematical equations describing groundwater flow are first presented, followed by the introduction of the inverse theory, the fundamental approximating functions of inversion, and the nonlinear solution techniques employed. Similar to [9], the Dupuit–Forchheimer assumption is adopted, which assumes negligible vertical flow. The aquifer can therefore be modeled in two-dimensions along the horizontal plane. For homogeneous aquifers, a “rule of thumb” was proposed by *Haitjema and Mitchell-Bruker* [10], defining conditions under which the Dupuit–Forchheimer assumption is applicable: $L \gg \sqrt{\frac{K_H}{K_V}H}$, where K_H and K_V are horizontal and vertical conductivities (K_H/K_V is 1.0 in our cases), L is distance between hydrogeological boundaries (i.e., lateral length of aquifer domains in this work), and H is aquifer thickness. All the test problems of this study are designed following this criterion, which results in negligible vertical flow, even when conductivity and recharge rates are inhomogeneous.

Under the Dupuit–Forchheimer assumption, steady state groundwater flow equation in a confined aquifer with source/sink effects is written as:

$$\frac{\partial}{\partial x} \left(Kb \frac{\partial h(x,y)}{\partial x} \right) + \frac{\partial}{\partial y} \left(Kb \frac{\partial h(x,y)}{\partial y} \right) + N(x,y) + Q\delta(x_0,y_0) = 0 \quad \text{on } \Omega \quad (1)$$

where $h(x,y)$ is hydraulic head [L], K is depth-averaged, locally isotropic hydraulic conductivity [L/T], $N(x,y)$ is areal source/sink rate [L/T] (only recharge is investigated), Q is pumping or injection rate at point (x_0,y_0) [L³/T] (wellbore radius is assumed zero), b is the saturated thickness, Ω is the solution domain. The aquifer problems in this work have a horizontal base which is set as the hydraulic head datum.

Model boundary conditions are a combination of no-flux and the Dirichlet-type boundary conditions:

$$h = g(x,y) \quad \text{on } \Gamma \quad (2)$$

where Γ is the Dirichlet-type domain boundary and $g(x,y)$ describes a set of specified heads on Γ .

Under the same Dupuit–Forchheimer assumption, steady state groundwater flow equation in an unconfined aquifer with source/sink effects is written as:

$$\frac{\partial}{\partial x} \left(Kh(x,y) \frac{\partial h(x,y)}{\partial x} \right) + \frac{\partial}{\partial y} \left(Kh(x,y) \frac{\partial h(x,y)}{\partial y} \right) + N(x,y) + Q\delta(x_0,y_0) = 0 \quad \text{on } \Omega \quad (3)$$

where $h(x,y)$ is unconfined aquifer hydraulic head which is identical to the saturated thickness for the chosen head datum. Similar to the boundary conditions of the confined aquifer, no-flow and Dirichlet boundaries are used.

2.1. Inverse method

The inversion method enforces two constraints: (1) global continuity of the hydraulic head and Darcy fluxes throughout the solution domain Ω ; (2) local conditioning of the inverse solution to observed hydraulic heads, fluxes, and/or flow rates. The continuity equations are written as:

$$\int R_h(\Gamma_j) \delta(p_j - \varepsilon) d\Gamma_j = 0, \quad j = 1, \dots, m \quad (4)$$

$$\int R_q(\Gamma_j) \delta(p_j - \varepsilon) d\Gamma_j = 0, \quad j = 1, \dots, m \quad (5)$$

where $R_h(\Gamma_j)$ and $R_q(\Gamma_j)$ are the residuals of a set of approximating functions of hydraulic head and Darcy fluxes at the j th cell boundary (or element interface) in the inversion grid, respectively. m is the total number of element interfaces. $\delta(p_j - \varepsilon)$ is the Dirac delta weighting function which samples the residual functions at a set of collocation points (p_j) on Γ_j . A value of 1.0 is assigned to this function; the continuity constraint is therefore strongly enforced. Both residual equations can be further expanded as:

$$R_h(\Gamma_j) = \bar{h}^i(\Gamma_j) - \bar{h}^k(\Gamma_j) \quad (6)$$

$$R_q(\Gamma_j) = \bar{q}^i(\Gamma_j) - \bar{q}^k(\Gamma_j) \quad (7)$$

where \bar{h} and \bar{q} are a set of proposed fundamental solutions of inversion (next). i and k denote cells in the inversion grid adjacent to the element interface Γ_j . For 2D inversion in a horizontal coordinate (x,y) , $\bar{q} = [q_x, q_y]$.

The fundamental solutions are conditioned at measurement locations:

$$\delta(p_j - \varepsilon)(\bar{h}(p_j) - h^o) = 0 \quad (8)$$

$$\delta(p_j - \varepsilon)(\bar{q}_x(p_j) - q_x^o) = 0 \quad (9)$$

$$\delta(p_j - \varepsilon)(\bar{q}_y(p_j) - q_y^o) = 0 \quad (10)$$

where p_j is a measurement point, h^o , q_x^o and q_y^o are the measured head and flux data, $\delta(p_j - \varepsilon)$ is a weighting function assigned to the equations to reflect the magnitude of the measurement errors. $\delta(p_j - \varepsilon)$ is generally proportional to the inverse of the error variance [26]. When measurement error is high, the weighting function is adjusted to be smaller; when measurements are error free, $\delta(p_j - \varepsilon) = 1$. In this study, for select aquifer problems, inverse results under both error-free and random measurement errors are investigated to evaluate the accuracy and instability of the inversion under increasing measurement errors.

Eqs. (9) and (10) are optional. When non-pumping conditions are investigated, these equations must be available to inversion to allow the unique and simultaneous estimation of the parameters (see discussion in Section 1). In these cases, subsurface fluxes

must be sampled and provided to inversion as observation data in addition to the hydraulic heads. However, under pumping conditions, the pumping and/or injection rates (Q) are considered known observation data. In these cases, Eqs. (9) and (10) are not used and the inverse solution is conditioned to the well rate(s) implicitly, as discussed below.

2.2. Fundamental solutions

A key component of the physical-based inverse method is the adoption and superposition of analytical flow solutions as the fundamental solutions of inversion [27]. The analytical solutions can be developed for homogeneous aquifers with uniform hydraulic conductivity and recharge rate; therefore the analytical solutions are applicable to describing flow in either individual grid cells or within individual hydrofacies zones with homogeneous parameters. Under this assumption, Eq. (1) of the confined aquifer becomes:

$$Kb \frac{\partial}{\partial x} \left(\frac{\partial h(x,y)}{\partial x} \right) + Kb \frac{\partial}{\partial y} \left(\frac{\partial h(x,y)}{\partial y} \right) + N(x,y) + Q\delta(x_0,y_0) = 0 \text{ on } \Omega_i \tag{11}$$

where K , N , b and Q are the hydraulic conductivity, recharge rate, saturated thickness of the homogeneous sub-domain (Ω_i), and pumping or injection rate inside Ω_i , respectively. For this equation, an analytical solution can be found:

$$\bar{h}(x,y) = a_1 + a_2x + a_3y + a_4xy - \frac{N}{2Kb} (a_5x^2 + (1 - a_5)y^2) + \frac{Q}{2\pi Kb} \ln \left((x - x_0)^2 + (y - y_0)^2 \right)^{\frac{1}{2}} \text{ on } \Omega_i \tag{12}$$

where a_1, a_2, a_3, a_4 and a_5 are a set of unknown coefficients. In Eq. (12), the first four terms reflect a background flow field due to large scale hydraulic boundary effect extending beyond Ω_i ; the 5th term describes flow induced from local recharge internal to Ω_i , and the last term describes pumping or injection induced change on the hydraulic head internal to Ω_i . Using Darcy's law, Darcy flux can be written as a set of analytical solutions:

$$\bar{q}_x(x,y) = -K \left(a_2 + a_4y - a_5x \frac{N}{Kb} + \frac{Q(x-x_0)}{2\pi Kb \left((x-x_0)^2 + (y-y_0)^2 \right)} \right) \text{ on } \Omega_i \tag{13}$$

$$\bar{q}_y(x,y) = -K \left(a_3 + a_4x - (1 - a_5)y \frac{N}{Kb} + \frac{Q(y-y_0)}{2\pi Kb \left((x-x_0)^2 + (y-y_0)^2 \right)} \right) \text{ on } \Omega_i \tag{14}$$

In inversion, K and N of the sub-domain are unknown parameters to be estimated. Eq. (11) is discretized over the inversion grid and the above coefficients become cell-wise constants: $\mathbf{x}^T = [a_1^l, a_2^l, a_3^l, a_4^l, a_5^l, K^l, N^l]$, $l = 1, \dots, M$ (number of grid cells), where \mathbf{x} is the inverse solution, the superscript T denotes transpose. In this work, a deterministic zoned parameterization is adopted to populate K and N in the aquifer. With this scheme, the number of equations to be solved are reduced and the solution becomes: $\mathbf{x}^T = [a_1^l, a_2^l, a_3^l, a_4^l, a_5^l, K^m, N^m]$, $l = 1, \dots, M$, $m = 1, \dots, R$ (number of hydraulic conductivity zones), $n = 1, \dots, H$ (number of recharge zones). Other than the imposed parameter zonations, however, no other prior information equations are used in inversion.

In the case of an unconfined aquifer subject to areal recharge to the water table, the flow equation of a locally homogeneous sub-domain (Ω_i) is:

$$K \frac{\partial}{\partial x} \left(h(x,y) \frac{\partial h(x,y)}{\partial x} \right) + K \frac{\partial}{\partial y} \left(h(x,y) \frac{\partial h(x,y)}{\partial y} \right) + N(x,y) + Q\delta(x_0,y_0) = 0 \text{ on } \Omega_i \tag{15}$$

where N and K are parameters that are constant in the sub-domain. Similarly, an analytical solution of hydraulic head in the sub-domain can be written as:

$$\bar{h}(x,y) = \left(a_1 + a_2x + a_3y + a_4xy - \frac{N}{K} (a_5x^2 + (1 - a_5)y^2) + \frac{Q}{2\pi K} \ln \left((x - x_0)^2 + (y - y_0)^2 \right) \right)^{\frac{1}{2}} \text{ on } \Omega_i \tag{16}$$

The analytical solutions of the Darcy flux are written as:

$$\bar{q}_x(x,y) = -K \frac{a_2 + a_4y - a_5x \frac{2N}{K} + \frac{Q(x-x_0)}{\pi K \left((x-x_0)^2 + (y-y_0)^2 \right)}}{2 \left(a_1 + a_2x + a_3y + a_4xy - \frac{N}{K} (a_5x^2 + (1 - a_5)y^2) + \frac{Q}{2\pi K} \ln \left((x - x_0)^2 + (y - y_0)^2 \right) \right)^{\frac{1}{2}}} \text{ on } \Omega_i \tag{17}$$

$$\bar{q}_y(x,y) = -K \frac{a_3 + a_4x - (1 - a_5)y \frac{2N}{K} + \frac{Q(y-y_0)}{\pi K \left((x-x_0)^2 + (y-y_0)^2 \right)}}{2 \left(a_1 + a_2x + a_3y + a_4xy - \frac{N}{K} (a_5x^2 + (1 - a_5)y^2) + \frac{Q}{2\pi K} \ln \left((x - x_0)^2 + (y - y_0)^2 \right) \right)^{\frac{1}{2}}} \text{ on } \Omega_i \tag{18}$$

Similar to the confined aquifer case, both the conductivity and the recharge rate are distributed in the model with a zoned parameterization.

For both confined and unconfined aquifers, this study first investigates problems without pumping or injection for which subsurface flux measurements must be sampled and provided to inversion as observation data. For these problems, the approximating functions can be obtained by setting $Q = 0$ in Eqs. (11)–(18). In addition, for problems where the underlying parameter variability(s) are unknown, inversion aims to estimate a set of equivalent or average parameters, e.g., equivalent conductivity K_{eq} and an average recharge rate (N). To estimate these parameters, the parameterization of the inverse method is slightly modified. For example, the measurement data can be sampled from a forward model with several hydraulic conductivity and recharge zones, but the inverse solution is parameterized as: $\mathbf{x}^T = [a_1^l, a_2^l, a_3^l, a_4^l, a_5^l, K_{eq}, \tilde{N}]$ (K and N are assumed homogeneous in the entire solution domain, thus the estimates are one equivalent conductivity and one average recharge rate), or $\mathbf{x}^T = [a_1^l, a_2^l, a_3^l, a_4^l, a_5^l, K1_{eq}, K2_{eq}; \tilde{N}1, \tilde{N}2]$ (two equivalent conductivity zones and two recharge zones are identified), etc.

This study next investigates situations with pumping and injection wells (in these problems, subsurface flux measurements are not needed). To represent pumping and injection induced changes on aquifer heads, Eqs. (11)–(18) are implemented in a hybrid formulation, where the well rate Q is specified to the well cell only (i.e., an inverse grid cell which hosts the well) but is zero outside the well cell. In this formulation, the size of the well cell must be adjusted so it is sufficiently large to accommodate a number of measured heads from nearby observation wells ~~with approximately the same values~~. The well size is also influenced by the proximity of the aquifer boundaries – if the influence from boundary conditions to pumping or injection is significant, the well cell dimension is accordingly reduced ~~but the hydraulic head approximating function is still approximately symmetric inside the cell~~. However, if the BC influence on pumping or injection is insignificant, the well cell can encompass a greater area. The adoption of

the hybrid formulation leads to significant computational savings, as the number of unknown coefficients is reduced compared to that using local grid refinement in order to capture high-gradient flows [27]. In inverting higher dimensional problems, local grid refinement at each well can lead to significantly larger equation systems, incurring higher computational costs.

For any of the confined or unconfined problems, once the inverse solution is found, i.e., both the estimated parameters and a set of recovered head and flux approximating functions (one set for each inversion grid cell), hydraulic head boundary conditions can be obtained by sampling the appropriate head functions at the boundary locations. Similarly, flux boundary conditions can be obtained by sampling the appropriate flux functions at the boundaries. In this work, all the inverted boundary conditions are presented as hydraulic head values.

2.3. Solution techniques

Eqs. (4) and (5) are written at all the m cell interfaces in the inversion grid; Eqs. (8)–(10) are written at the locations where the measurement data are available. The inverse system of equations is assembled, which can be under-determined, exact, or over-determined (for the aquifer problems of this study, all systems of equations are over-determined, because under-determined problems generally yield poor solutions). The coefficients of the fundamental solutions are the unknowns, along with the parameters to be estimated. Due to the nonlinearity in the fundamental solutions, all equations are nonlinear and are solved with two gradient-based local optimization algorithms, i.e., Levenberg–Marquardt and Trust-Region-Reflective. Both algorithms are implemented in the Matlab nonlinear solver, *lsqnonlin*, which solves a nonlinear least-squares problem of the form (The Mathworks, 2012):

$$\underset{\mathbf{x}}{\text{mix}} f(\mathbf{x})_2^2 = \underset{\mathbf{x}}{\text{mix}} (f_1(\mathbf{x})^2 + f_2(\mathbf{x})^2 + \dots + f_n(\mathbf{x})^2) \quad (19)$$

where \mathbf{x} is solution of the system of equations and n is number of equations. With *lsqnonlin*, constraints can also be placed on the values of \mathbf{x} , e.g., enforcing positive values for K and the recharge rates.

The above optimization algorithm requires that initial guess of \mathbf{x} be provided. For the confined aquifer cases, the initial guess (\mathbf{x}_0) was given an arbitrary set of values. For well-posed problems (i.e., measurement data are of sufficient density and accuracy), numerical experiments with different \mathbf{x}_0 yielded identical inverse results. However, for the unconfined aquifer cases, arbitrary \mathbf{x}_0 values can lead to a non-convergence of the iterative solver. These problems have a greater degree of nonlinearity compared to the confined problems. Thus, the initial guess (\mathbf{x}_0) was computed by minimizing Eqs. (8)–(10) with an one-cell inversion grid (the continuity equations were excluded from the system of equations). The values obtained were then used as the initial guess for full inversion. This approach is similar to fitting an analytical model to an equivalent homogeneous media of a heterogeneous aquifer, and therefore \mathbf{x}_0 values reflect a set of equivalent parameters. With this treatment, inversion yielded stable results for all the unconfined problems tested.

In generating \mathbf{x}_0 , the hydraulic conductivity or recharge parameterization needs not be identical to that adopted in full inversion. For example, we can estimate a single conductivity or a single recharge rate even if the full inversion estimates a number of conductivities and recharge rates. These initial guesses, in effect, provide a set of rough averages for these parameters. Numerical experimentations indicate that when the problem is well conditioned, starting the full inversion with different \mathbf{x}_0 yields identical outcomes. Another benefit of the reduced parameterization

approach is that reasonable \mathbf{x}_0 values can be generated with few measurement data, which is useful in field reconnaissance situations where initially only limited measurements are available.

The inverse method, similar to the objective-function based inversion techniques, may suffer ill posedness when insufficient and/or noisy data are supplied to condition the solution. Thus, (1) solution may not exist; (2) solution may not be unique; (3) solution may be unstable. Generally, the accuracy of the inverse method depends on the location, quantity, and quality (accuracy) of the observation data. Given sufficient and accurate data which yield exact or over-determined systems of equations, the inverse method becomes well-posed, leading to fast, stable, and accurate solutions. In this work, sufficient data (of varying qualities) are provided to inversion, leading to a set of over-determined equations.

3. Results

In this work, inversion quality is determined by comparing the estimated parameters (hydraulic conductivities, recharge rates) and the recovered hydraulic head field (including the boundary head) to those of several synthetic “true” models. These forward problems are used to generate the “true” observation data under a set of true model BC. These problems are created with detailed finite-difference forward flow simulations by MODFLOW2000, which is implemented in the software *Groundwater Vista*. However, *Vista* adopts the English units. In the following paragraphs, dimensions for all relevant quantities implicitly assume a consistent set of units (head in ft, K and N are in ft/d, q in ft³/d), thus units of some parameters are not labeled. The synthetic problems employ either a regular or irregular computational domain, as explained below.

For the regular-domain problems, seven confined aquifer cases are investigated. For cases 1–6, pumping and injection wells are not used (all wells are observation wells), for which a set of K s and N s are estimated. For cases 5 and 6, equivalent K_{eq} and average \bar{N} are estimated to evaluate the issues associated with model structure errors. For case 7, a confined problem is solved with one pumping well and one injection well. Next, three unconfined aquifer cases are investigated, without pumping and injection wells. For one of the cases, equivalent parameters are also estimated.

For the irregular-domain problems, one confined aquifer problem is inverted first, without and with pumping and injection wells. An unconfined problem is inverted next, without and with wells.

For the select cases above, stability tests are conducted to evaluate the accuracy of the outcomes under increasing magnitude of the head measurement errors. As the true model is a solution of the finite difference method (FDM), measurements sampled from this solution (“true heads”) are considered approximately error-free, but they do contain minor discretization and solution errors. To impose measurements errors, hydraulic heads computed by the FDM are corrupted by noise: $h^m = h^{FDM} \pm \Delta h$, where h^m is the measured head provided to inversion, h^{FDM} is the head sampled from the FDM, and Δh is the measurement error or noise. The highest noise imposed on the true heads is $\pm 5\%$ of the total head variation. These variations are fairly large, i.e., Δh of $\pm 5\%$ results in a set of head measurements that fluctuate over an interval that is 10% of the total head change in the system. The larger errors are imposed mainly to test stability of the inversion. We assume that only hydraulic head data are subject to errors. Measurements of Darcy fluxes, when sampled from the FDM model, are not corrupted by noises. For the cases investigating pumping tests, the true well rates are provided to inversion without errors.

3.1. Regular domain

3.1.1. Confined aquifer cases

For the first 4 cases, the FD forward models (50 × 50 grid; $L_x = 1000$ ft, $L_y = 1000$ ft) are a suite of numerical solutions of two-dimensional groundwater flow in a confined aquifer driven by various leakage rates under otherwise similar boundary conditions (Fig. 1). True parameter values of each model are presented in Table 1.

For cases 1 and 2, 24 heads were measured at 24 fictitious observation well locations along a quasi-regular grid. A single flux component (q_y^0) was measured in the top leftmost corner of the model. For case 3, the same 24 head measurements were made, but 4 flux components were measured randomly. Compared to cases 1, 2, and 4, where K variation ranges from small to modest (i.e., the highest K_{max}/K_{min} is 100), case 3 investigates strong aquifer K variation with a K_{max}/K_{min} of 10,000. For case 4, 36 heads in a quasi-regular pattern and 1 flux at the top leftmost corner of the model were measured. In this case, more parameters are estimated compared to the other cases (Fig. 1c). Accordingly, more measurement data were provided to inversion.

For all cases, when error-free head data are used to condition the inverse solutions, the estimated conductivities and recharge rates are close to those of the true models, i.e., the absolute estimation error (i.e., $|K_{true} - K_{est}|$) is ~5% of the true parameter values, with the largest error of ~8%. When observed heads with ±1% measurement error are used, the estimated conductivities and recharge rates are still reasonable, with the absolute relative error (i.e.,

$|K_{true} - K_{est}|/K_{true} \times 100\%$) up to 14%. When the head error is ±5%, parameter estimation becomes less accurate – the maximum absolute relative error is now up to 90%. However, all cases tested yield stable solutions. It is important to point out that all the inverse solutions are computed with small grids (Table 1). Therefore, the inversion systems of equation are accordingly small, leading to high computation efficiency. Typically, one inversion run takes about 1–3 s to complete on a PC laptop.

In case 3, K_{max}/K_{min} tested is 10,000. Fig. 2 presents its computational domain and the comparison between the inverted heads and the true FD heads along a 1D profile which extends from the inlet boundary to the outlet boundary. With a small (2 × 2) grid, the inverted heads are very accurate throughout this profile. However, when the head measurement error reaches ±5%, the inverted heads become less accurate. In this case, the inverted head profile overestimates the true head profile by ~10% in the low-conductivity K_1 zone, but head profile is accurate in the high-conductivity K_2 zone. For all the error levels tested, the inversion is stable. Fig. 3 further compares the hydraulic head contours for the three tested error levels. This comparison suggests good to fair accuracy in the head recovery throughout the computational domain. The accuracy degrades with increasing head measurement errors, as expected.

Two additional confined aquifer problems are solved. Case 5 has a computational domain, grid size, K values, and observation locations that are identical to those of case 4. However, in simulating its forward model, N is specified zero throughout the model domain. Without any measurement errors, the inversion yields: $K_1 = 1$, $K_2 = 82.8$ and $K_3 = 7.7$, $N_1 = -1.19 \times 10^{-6}$,

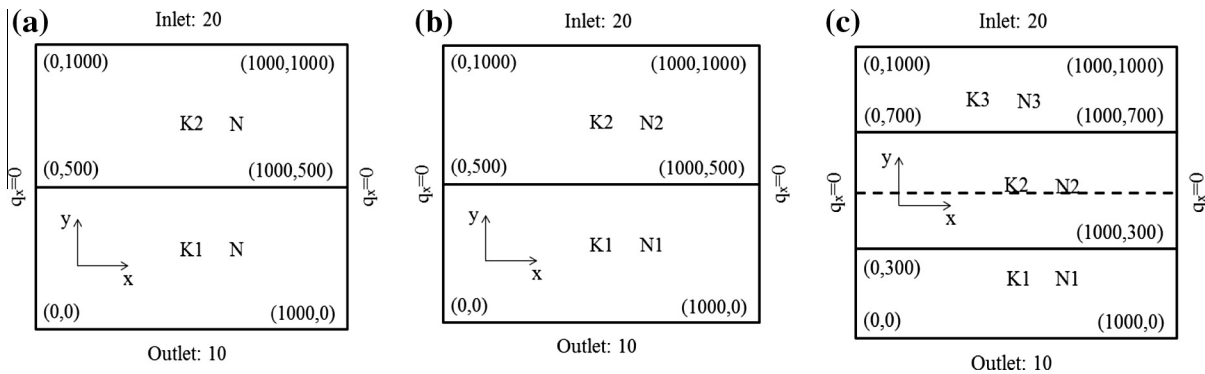


Fig. 1. Computational domain for confined aquifer inversion: (a) case 1, (b) cases 2 and 3, and (c) case 4. (See text for the description of case 5.) The dashed line in the middle of (c) indicates the new parameterization adopted by case 6 (upper zone: K_{2eq} , \tilde{N}_2 ; lower zone: K_{1eq} , \tilde{N}_1). For all cases, the Dirichlet boundary condition is shown as “Inlet” head and “Outlet” head. All length units are in ft.

Table 1
Inversion outcomes for cases 1–4 (confined aquifer). The estimated K and N parameters are in unit of ft/d.

	True parameters	Estimated parameters (no error)	Estimated parameters (±1% head error) (±0.1 ft)	Estimated parameters (±5% head error) (±0.5 ft)	Inverse grid	Measured data*
Case 1	$K_1 = 1; K_2 = 10$ $N = 10^{-4}$	$K_1 = 0.99; K_2 = 9.5$ $N = 9.28 \times 10^{-5}$	$K_1 = 0.91; K_2 = 8.89$ $N = 8.6 \times 10^{-5}$	$K_1 = 0.6; K_2 = 1.84$ $N = 4 \times 10^{-5}$	2 × 2	24h + 1 q_y
Case 2	$K_1 = 1; K_2 = 10$ $N_1 = 10^{-4}$ $N_2 = 5 \times 10^{-4}$	$K_1 = 1; K_2 = 10.04$ $N_1 = 1.01 \times 10^{-4}$ $N_2 = 5.03 \times 10^{-4}$	$K_1 = 0.69; K_2 = 6.79$ $N_1 = 9.84 \times 10^{-5}$ $N_2 = 3.41 \times 10^{-4}$	$K_1 = 0.14; K_2 = 1.1$ $N_1 = 4.06 \times 10^{-5}$ $N_2 = 5.05 \times 10^{-5}$	2 × 2	24h + 1 q_y
Case 3	$K_1 = 0.1;$ $K_2 = 1000$ $N_1 = 10^{-4}$ $N_2 = 10^{-3}$	$K_1 = 0.102;$ $K_2 = 913.9$ $N_1 = 1.01 \times 10^{-4}$ $N_2 = 9.9 \times 10^{-4}$	$K_1 = 0.095;$ $K_2 = 460.12$ $N_1 = 1.12 \times 10^{-4}$ $N_2 = 5.99 \times 10^{-4}$	$K_1 = 0.036;$ $K_2 = 19.16$ $N_1 = 7.29 \times 10^{-5}$ $N_2 = 1.16 \times 10^{-5}$	2 × 2	24h + 4 q_y
Case 4	$K_1 = 1; K_2 = 100$ $K_3 = 10$ $N_1 = 10^{-4}$ $N_2 = 10^{-3}$ $N_3 = 5 \times 10^{-4}$	$K_1 = 1; K_2 = 102.64$ $K_3 = 10.37$ $N_1 = 1.01 \times 10^{-4}$ $N_2 = 10^{-3}$ $N_3 = 5.19 \times 10^{-4}$	$K_1 = 0.99; K_2 = 99.9$ $K_3 = 10.13$ $N_1 = 9.95 \times 10^{-5}$ $N_2 = 9.12 \times 10^{-4}$ $N_3 = 4.94 \times 10^{-4}$	$K_1 = 0.43; K_2 = 0.17$ $K_3 = 0.02$ $N_1 = 5.31 \times 10^{-5}$ $N_2 = 5.6 \times 10^{-6}$ $N_3 = 1.25 \times 10^{-6}$	2 × 3	36h + 1 q_y

* ‘h’ Denotes heads; q_x or q_y denote flux components.

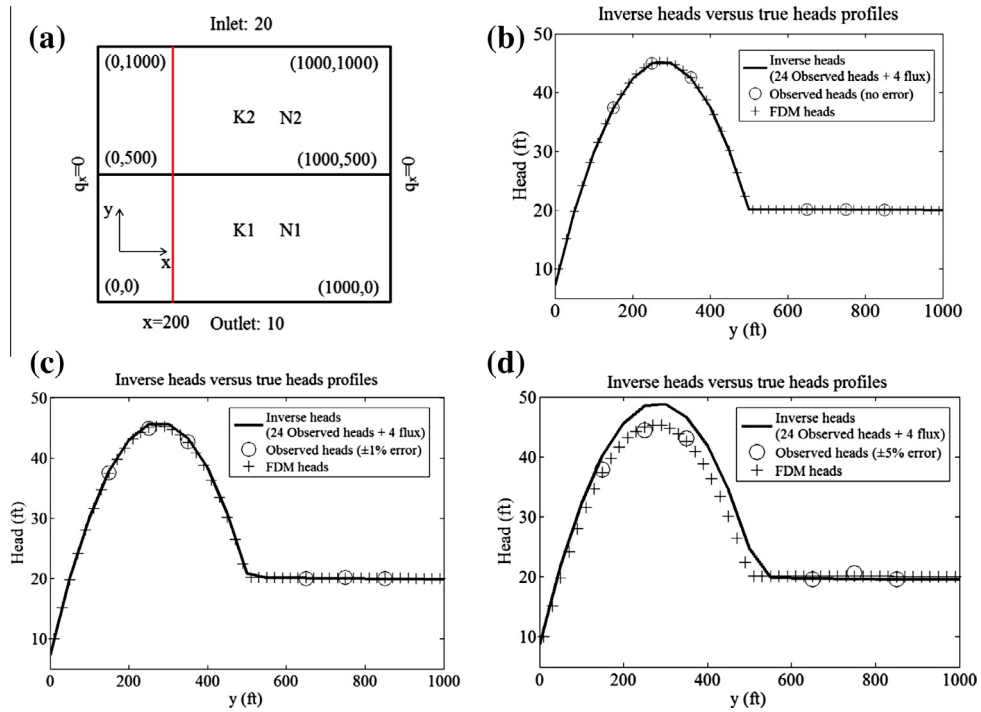


Fig. 2. Inversion outcomes of case 3: (a) computational domain with a line at $x = 200$ ft indicating the location where the inverted head is compared to the true FD head. Head profiles along the line when (b) the measured heads are error-free. (c) Measured heads contain $\pm 1\%$ error. (d) Measured heads contain $\pm 5\%$ error. Location of the measured heads is also indicated (circles).

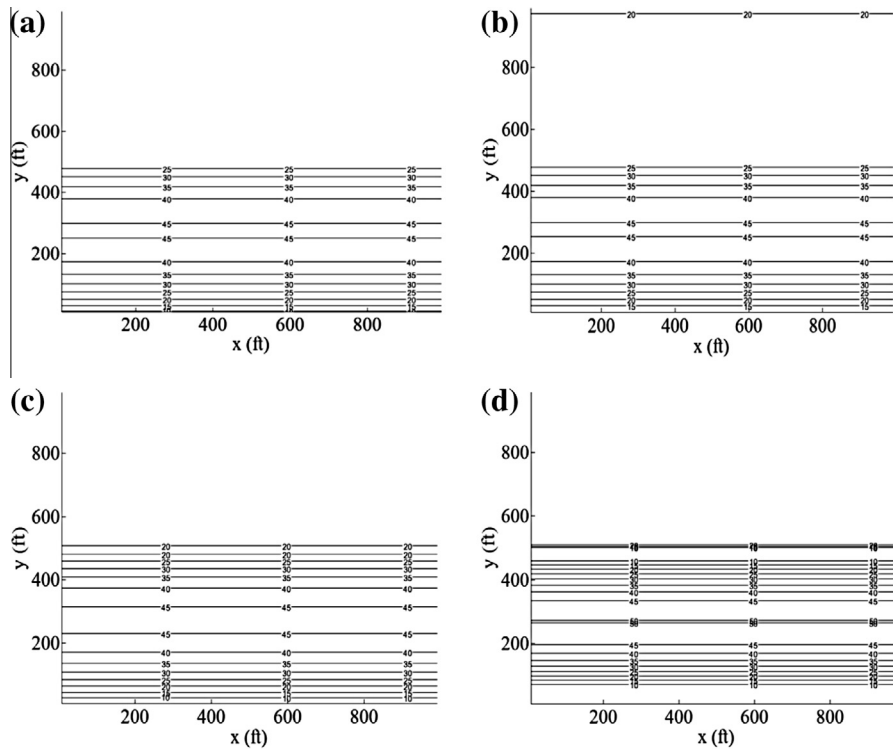


Fig. 3. Hydraulic head contour map of case 3. (a) Head contour map of the FDM; (b) inverted head given error-free measured heads; (c) inverted head given measured heads with $\pm 1\%$ errors; (d) inverted head given measured heads with $\pm 5\%$ errors.

$N2 = 1.92 \times 10^{-5}$ and $N3 = -1.57 \times 10^{-7}$. The estimated recharge rates are close to zero, while the conductivities are close to the true values. Clearly, the inversion method is robust and is insensitive to model structure error, i.e., inverse parameterization complexities

the true parameter field. The inversion outcomes can reveal spurious parameters (i.e., recharge rates) while the simultaneous estimation of the non-spurious parameters (i.e., conductivities) is not affected.

Case 6 has the same forward model and observation data as case 4, except its conductivity and recharge parameterizations are modified to those of a two-zoned model (see the dashed line in Fig. 1c; in inversion, a 2×2 grid is used, which honors the lateral interface between the two zones). Clearly, this inverse parameterization simplifies the true parameter field, resulting in a model structure error. Given error-free observed data, the estimated conductivities and the recharge rates are: $K1 = 1.13$, $K2 = 13.79$, $N1 = 2.08 \times 10^{-4}$ and $N2 = 1.4 \times 10^{-3}$. These values are fairly close to the analytical equivalent conductivities and recharge rates that are independently computed based on the true parameters: $K1_{eq} = 1.66$, $K2_{eq} = 15.6$, $\bar{N}1 = 4.6 \times 10^{-4}$ and $\bar{N}2 = 7 \times 10^{-4}$. Because the inverse method is physical-based, the estimated two-zoned parameters are physically meaningful, as they reflect equivalent or average parameters. Deviation between the two sets of parameters is believed to be a result of (1) limited measurement data, (2) finite arithmetic in numerical inversion, and (3) inversion is for a finite domain while analytical conductivities are strictly calculated for an infinite domain.

Case 7 has a set of pumping and injection wells that operate at the same rate, i.e., 25 ft³/d. Both wells are placed close to the model boundaries (Fig. 4), and as a result, drawdown at the wells is significantly influenced by the characteristics of the boundary conditions (recharge effect, which can mask the boundary effect, is not modeled). Two sets of true BC are tested: a constant head of 2000 ft is specified to the entire model boundary (Fig. 4a–c); and a similar boundary is specified except the left-hand-side model is no flow (Fig. 4d–f). From the forward model, 144 hydraulic heads are sampled. The inversion outcomes are presented as a set of recovered heads against the true FDM heads along two profiles (AB, CD), both of which are placed close to the wells. For the two sets of BC, the head recovery is excellent at both profiles. Under the first set of BC (specified constant head), asymmetry in the drawdown that is predicted by the forward model at locations

close to the boundaries (i.e., the bottom left corner and the top right corner) is captured very well by the inverse solution. Similarly, under the second set of BC (specified constant head and a no-flow), asymmetry in the forward solution is also captured by inversion: due to the no-flow boundary at the left-hand-side of the model, both solutions display lower heads that fall perpendicular to the no-flow boundary – the head values here are lower than the heads on the other side of the well where drawdown is not significantly influenced by the right-hand-side boundary which lies far from the well. Clearly, for problems with wells, the inverse method can account for the effects of different types of boundaries on drawdowns, while many existing methods cannot. For both BC, the estimated parameters are also presented showing good accuracy (Table 2), when error-free measurements are provided to inversion.

3.1.2. Unconfined aquifer cases

The forward models are simulated with a 3D FDM ($50 \times 50 \times 20$) in a domain that is $1000 \times 1000 \times 40$ ft³ (Fig. 5).

Table 2

Inversion outcomes for case 7 (confined aquifer). The estimated K are in unit of ft/d. BC1 refers to constant specified heads along the entire model boundary; BC2 refers to a similar set of the model boundary conditions, except the left-hand-side model is no-flow.

	True parameters	Estimated parameters (no error)	Inverse grid	Measured data
BC1	$K1 = 1$ $K2 = 10$	$K1 = 1.08$ $K2 = 13.4$	12×12	144 heads + pumping + injection rates
BC2	$K1 = 1$ $K2 = 10$	$K1 = 1.09$ $K2 = 12.4$	12×12	144 heads + pumping + injection rates

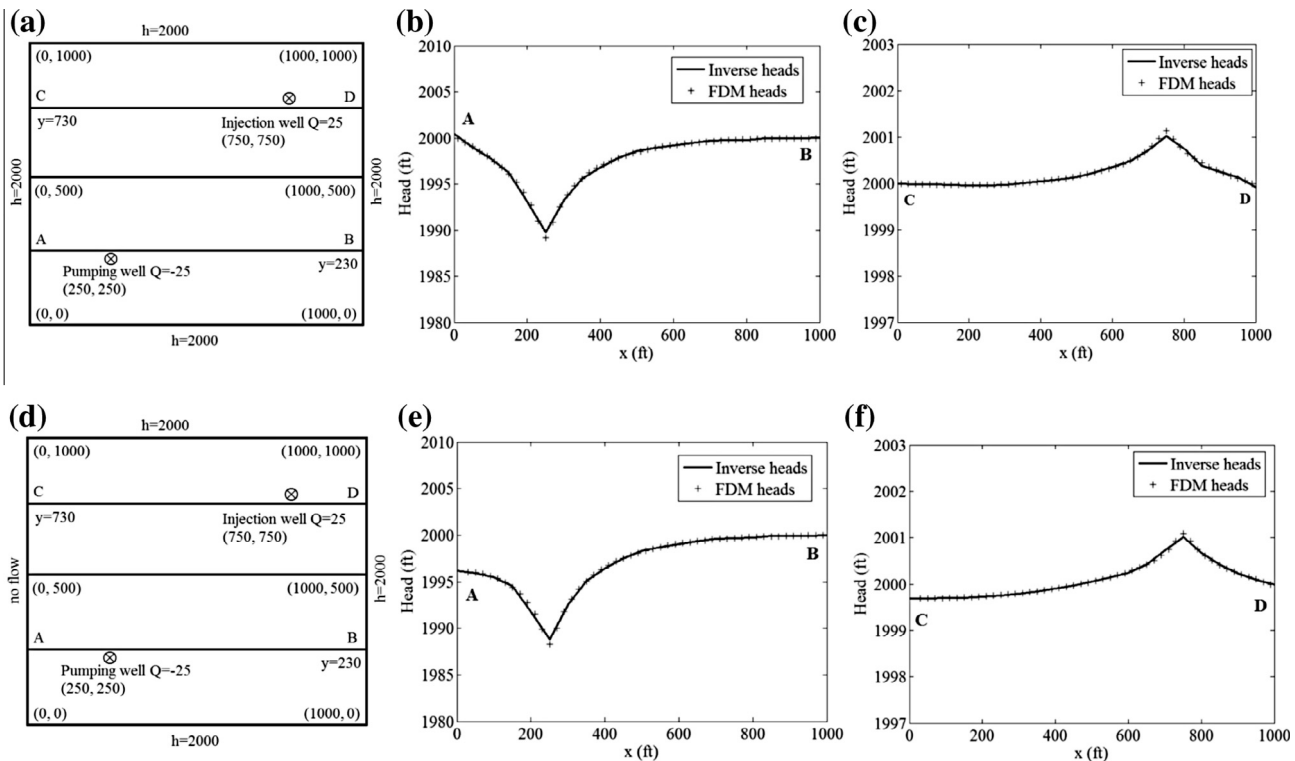


Fig. 4. Confined problem (case 7) with pumping and injection wells. (a) Location of the wells and true model BC; (b) true FDM heads and recovered heads along profile AB; (c) true FDM heads and recovered heads along profile CD; and (d–f) describe a similar problem except the left-hand-side boundary is no-flow.

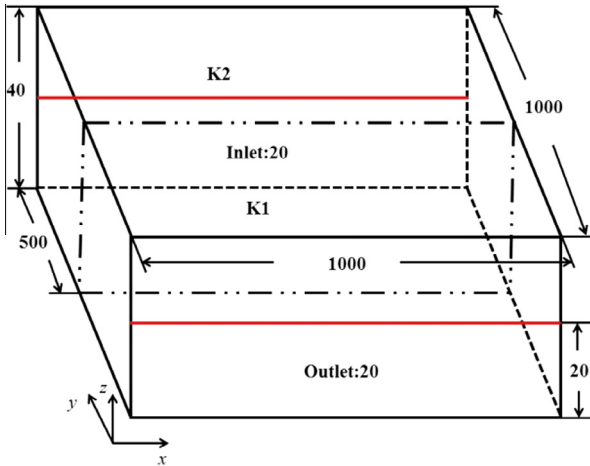


Fig. 5. Computational domain of an unconfined aquifer. Boundary conditions of this problem are shown: no-flow on the left, right, and bottom boundaries; a fixed head of 20 ft is specified to the front and back faces (red lines). A uniform recharge rate is specified to the model top. Conductivity of case 1 is uniform. Case 2 has two conductivity zones: K_1 in the front half of the model domain; K_2 in the back half. (For interpretation of the references to color in this figure legend, the reader is referred to the web version of this article.)

Inversion results for two different cases are presented in [Table 3](#). Both cases use a 2D inverse grid of 2×2 cells. Case 1 has a uniform K and a uniform N . The observation data are sampled from 24 observation wells on a horizontal plane at $z = 10$ ft (this sampling pattern is semi-regular). Case 2 has two conductivity zones and the same uniform N . The same observation data are sampled. For both cases, inversion results are excellent when the head measurement error is either zero or very small. As expected, accuracy degrades with increasing errors. For case 2, [Fig. 6](#) shows a comparison of the head contours of the true model and the inversion results under increasing measurement errors. The inverse results are stable in all of these problems. The small inversion grid again yields small systems of equations, for which the computational speed is similar to that observed when inverting the confined aquifer problems.

In addition, model structure error is investigated for another unconfined problem. The true 3D model is similar to [Fig. 5](#), except three different parameter zones are defined where the domain is divided in the y -direction as: ($K_1 = 1, N_1 = 2.0 \times 10^{-4}$) with $y \in [0, 300]$, ($K_2 = 25, N_2 = 5.0 \times 10^{-3}$) with $y \in [300, 700]$, and ($K_3 = 5, N_3 = 1.0 \times 10^{-3}$) with $y \in [700, 1000]$. In the 2D inverse formation, two parameter zones are defined ($y \in [0, 500]$ and $y \in [500, 1000]$), i.e., simplifying model structure error. A 2×2 inverse grid is used.

Table 3

Inversion outcomes for cases 1 and 2 (unconfined aquifer). The estimated K and N parameters are in unit of ft/d.

	True parameters	Estimated parameters (no error)	Estimated parameters ($\pm 1\%$ head error) (± 0.01 ft)	Estimated parameters ($\pm 5\%$ head error) (± 0.05 ft)	Inverse grid	Measured data
Case 1	$K = 1$ $N = 10^{-4}$	$K = 0.99$ $N = 9.76 \times 10^{-5}$	$K = 1.16$ $N = 1.15 \times 10^{-4}$	$K = 23.36$ $N = 2.3 \times 10^{-3}$	2×2	$24h + 1q_y$
Case 2	$K_1 = 1; K_2 = 10$ $N = 10^{-3}$	$K_1 = 1; K_2 = 9.7$ $N = 10^{-3}$	$K_1 = 0.78; K_2 = 7.8$ $N = 7.79 \times 10^{-4}$	$K_1 = 0.21; K_2 = 2.1$ $N = 2.1 \times 10^{-4}$	2×2	$24h + 1q_y$

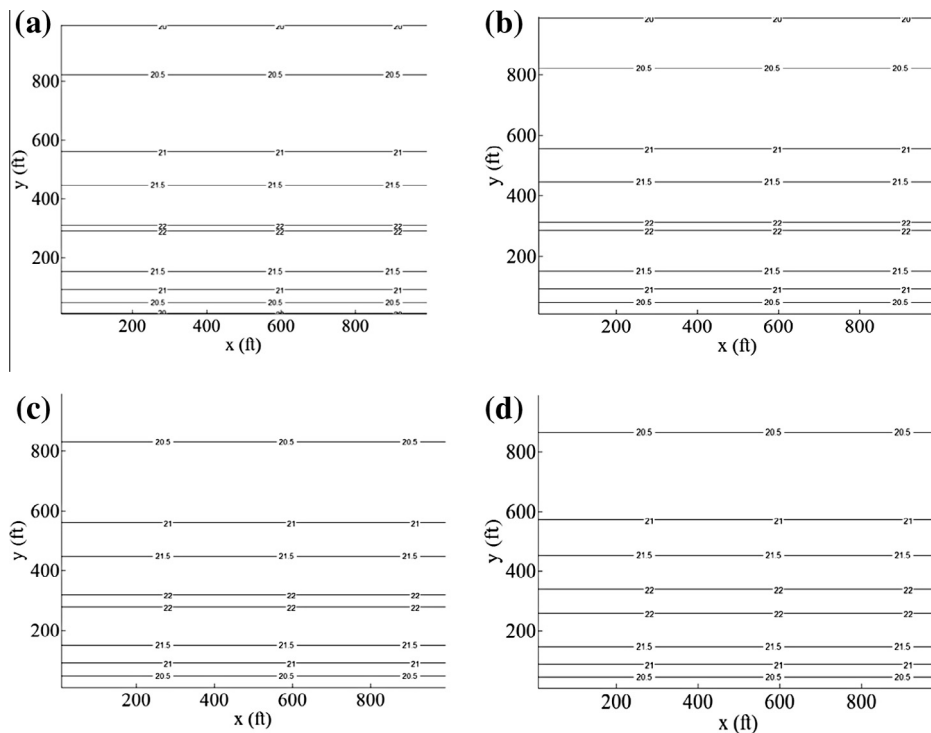


Fig. 6. Head contour map of the unconfined aquifer (case 2): (a) FDM true model; (b) inversion result with error-free measured heads; (c) inversion result with $\pm 1\%$ head measurement errors; (d) inversion result with $\pm 5\%$ errors.

Based on 24 observed heads and 2 observed flux components sampled from the forward model, the inversion obtains: $K1 = 1.08$; $K2 = 7.24$; $N1 = 1.0 \times 10^{-3}$; $N2 = 5.5 \times 10^{-3}$. In comparison, the equivalent conductivities and the average recharge rates for this 2-zoned problem can be computed analytically as: $K1_{eq} = 1.62$; $K2_{eq} = 7.35$; $\tilde{N}1 = 2.1 \times 10^{-3}$; $\tilde{N}2 = 2.6 \times 10^{-3}$. Again, the comparison is reasonable. The inverse solution also recovers the hydraulic head field which is close to the FDM-computed true head field (not shown).

3.2. Irregular domain

The inverse method is proven accurate and robust when simple computational domains are investigated. In this section, for a

confined and then an unconfined aquifer problem, inversion of more complex aquifer geometries and flow patterns is of interest.

3.2.1. Confined aquifer

First, a confined problem without pumping and injection wells is investigated. For this problem, the FDM true model is 2D, whose grid, parameters, and associated boundary conditions are shown in Fig. 7a. This model includes 4 conductivity zones and a uniform recharge (or leakage) rate to the top of the aquifer. The true boundary conditions consist of a no-flow boundary (solid line) and a specified head boundary (dashed line; specified head values shown). This parameterization pattern is assumed known in inversion, which uses a fairly coarse grid (Fig. 7b). The head and flux measurement locations at observation wells are also shown (Fig. 7b):

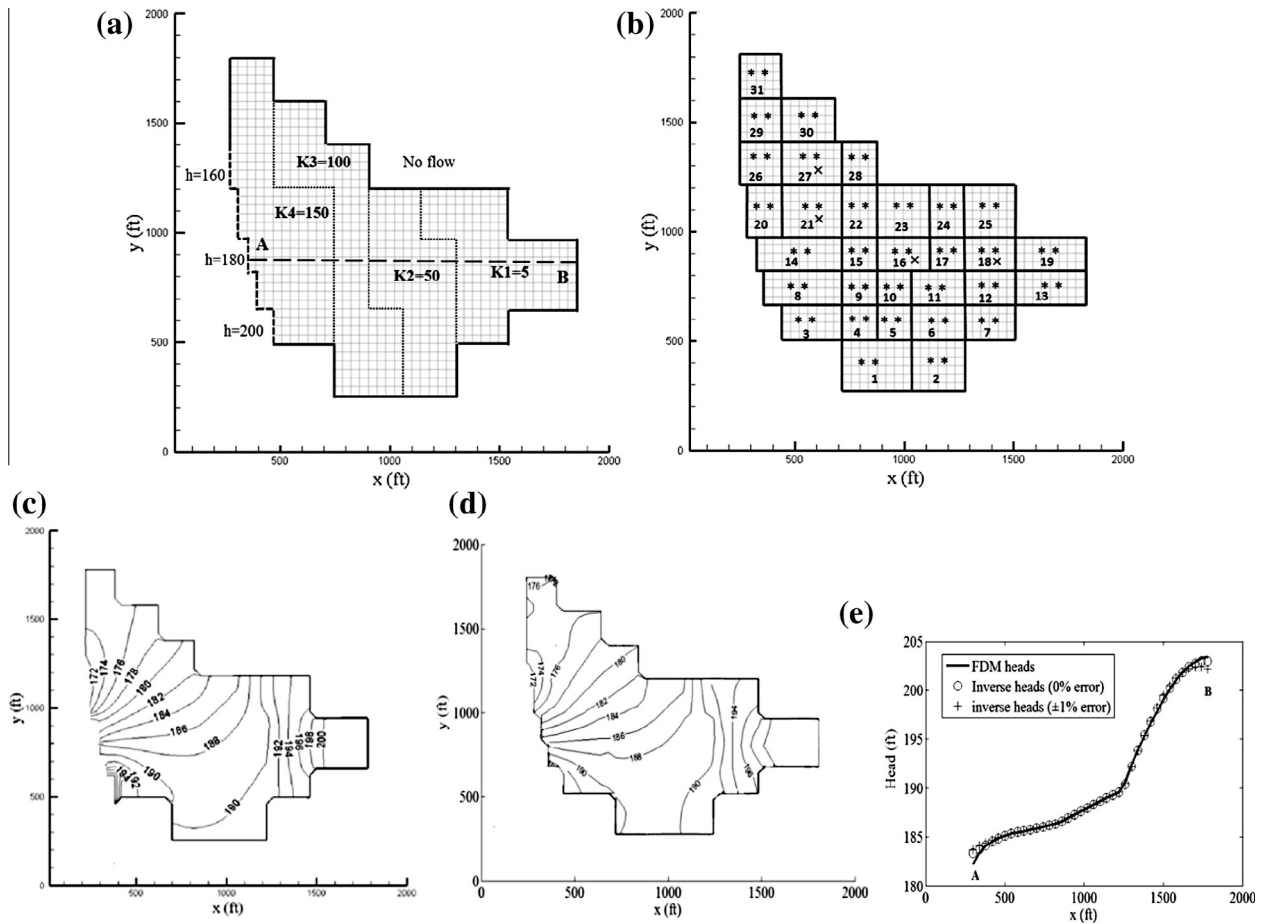


Fig. 7. (a) FDM true model of a confined aquifer with four conductivities ($K1 = 5$, $K2 = 50$, $K3 = 100$, $K4 = 150$) and $N = 0.0005$. Location of a profile, AB, is shown at $y = 860$ ft. The FDM grid is shown by the grey lines. (b) Inverse grid (31 cells) and the measurement location (* denote 62 sampled heads; x denote 4 sampled q_x). (c) Head contours predicted by the true model. (d) Head contours predicted by inversion with 31 cells when head measurement error is $\pm 1\%$. The same contour levels as those of the true model are used. (e) Head profiles predicted along AB by the true model and using inversion (31 cells) when measurement errors are increased.

Table 4

Inversion outcomes of an irregularly shaped confined aquifer, without and with pumping/injection wells. The estimated K and N parameters are in unit of ft/d.

	Hydraulic conductivities				Recharge	Number of inversion cells
	K1	K2	K3	K4	N	-
True parameters	5	50	100	150	5×10^{-4}	-
Without pumping/injection 0% (0)	5.4	28.9	105.3	130.7	3.1×10^{-6}	19
Without pumping/injection 0% (0)	4.7	43.4	107.1	141.4	4.1×10^{-4}	31
Without pumping/injection $\pm 1\%$ (± 0.4 ft)	5.5	47.1	112.6	142.8	4×10^{-4}	31
With pumping/injection 0% (0)	5.8	58	124	167	5.0×10^{-4}	31
With pumping/injection $\pm 0.25\%$ (± 0.1 ft)	6.1	58	134	169	4.7×10^{-4}	31

62 heads and 4 q_x are sampled. The FDM head solution is shown in Fig. 7c. For the given measurement data (with $\pm 1\%$ error added), the inverted head field is shown in Fig. 7d. Head profiles of the FDM and the inverted solutions (under both error-free and $\pm 1\%$ error) are plotted along profile AB (Fig. 7e). Comparison between the true and inverted head contours or profiles is excellent. Moreover, the estimated parameters are shown in Table 4. Initially, a coarse inverse grid with 19 cells is used (not shown), which results in up to 22% absolute relative error in K estimation and $\sim 99\%$ absolute relative error in N estimation, given error-free measurements. The inverse grid is then refined to contain 31 cells (Fig. 7b), where model regions with high gradients of the observed heads are refined. Given the same error-free measurements, inversion results improved significantly: $\sim 9\%$ absolute relative error in K estimation and $\sim 18\%$ absolute relative error in N estimation. Again, as was observed for inverting the regular domain problems, increasing head measurement errors lead to reduced inversion accuracy.

Next, for the same confined problem, a pumping well and an injection well are added (Fig. 8a). As in the previous problem, the same set of 62 observed heads are sampled. Flux measurements are not taken. The two well rates are considered known measurements. Inversion adopts the same 31-cell grid (Fig. 7b). Because of the non-zero recharge rate and the particular boundary conditions adopted (i.e., hydraulic head is more elevated in the southern portion of the model), pumping or injection induced head changes are not significant – the local cone of depression (or the elevated heads near the injector) is not obvious at the wells. However, the effect of

recharge and wells are implemented in the hybrid formulation, as explained before. In this case, the size of well cells at both the pumping and injection wells can be fairly large, i.e., pumping in cell 11, injection in cell 21 (Fig. 7b), without the need to locally refine the grid. Despite the increased complexity compared to the same problem inverted above (Fig. 7), both the head recovery (Fig. 8c and d) and parameter estimation (Table 4) are accurate when measurement errors are small.

3.2.2. Unconfined aquifer

The equation describing unconfined aquifer flow is more non-linear compared to that of the confined aquifer. It is therefore of interest to compare their estimation accuracy using the inverse method. First of all, under non-pumping conditions, an irregular aquifer with 4 K zones (of the same K values as those of the previous confined aquifer) and a uniform recharge rate to the top of the water table is analyzed (Fig. 9a). The true model is 3D ($50 \times 50 \times 20$ grid; $1000 \times 1000 \times 40$ ft³; Inactive cells are used to delineate the irregular domain shape); its head contours are shown in Fig. 9b at $z = 12$ ft. As in inverting the previous confined problems, the same 2D inverse grid with 31 cells is used. Location of the measured data is also the same, except they are now sampled at $z = 12$ ft. Without any measurement errors, the inverted heads are close to the true heads, with the exception of minor deviations in some local areas. The estimated parameters are close to the true parameters (Table 5). Next, the same observed heads are used in inverting the unconfined problem where a pair of injection and pumping

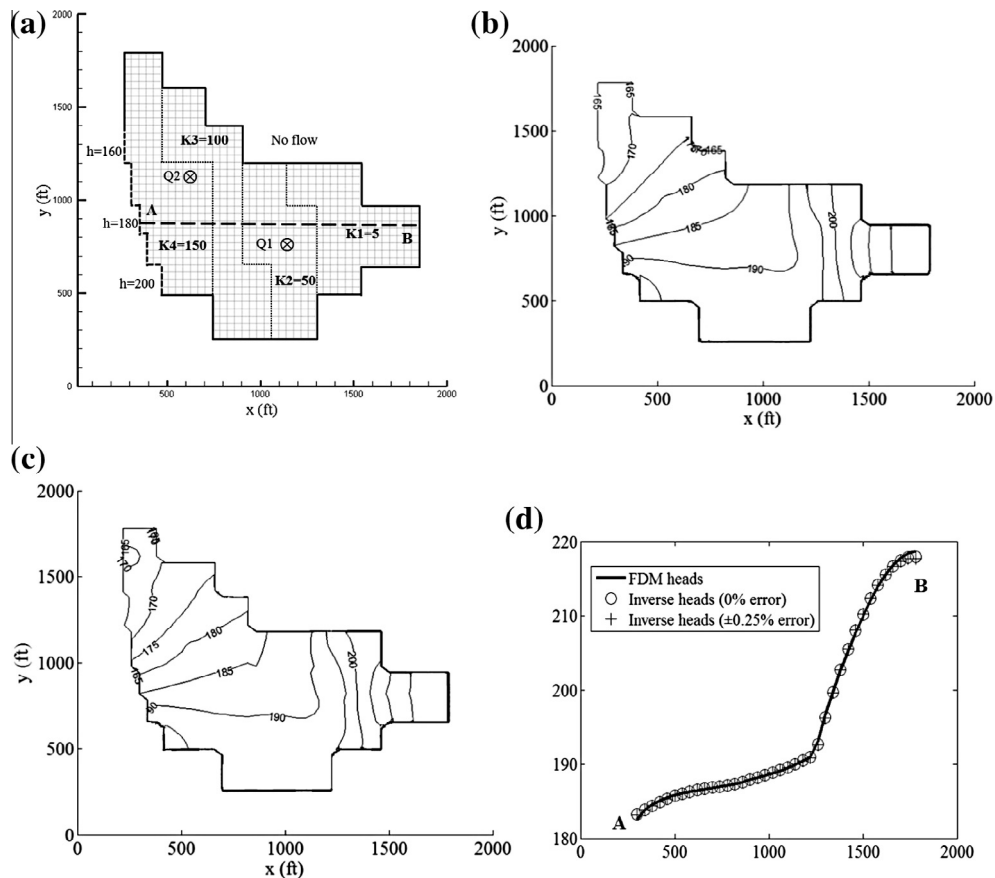


Fig. 8. Confined problem with a pair of pumping and injection wells: $Q1 = -300$ (pumping well) at (1100, 740) and $Q2 = 300$ (injection well) at (540, 1100). (a) FDM true model with four conductivities ($K1 = 5, K2 = 50, K3 = 100, K4 = 150$) and $N = 0.0005$. Location of a profile, AB, is shown at $y = 860$ ft. In the forward model, to accurately compute the drawdowns, LGR (not shown) is performed at both well locations. (b) Head contours predicted by the true model. (c) Head contours predicted by inversion with 31 cells when head measurement error is $\pm 0.25\%$. The same contour levels as those of the true model are used. (d) Head profiles predicted along AB by the true model and using inversion when measurement errors are increased.

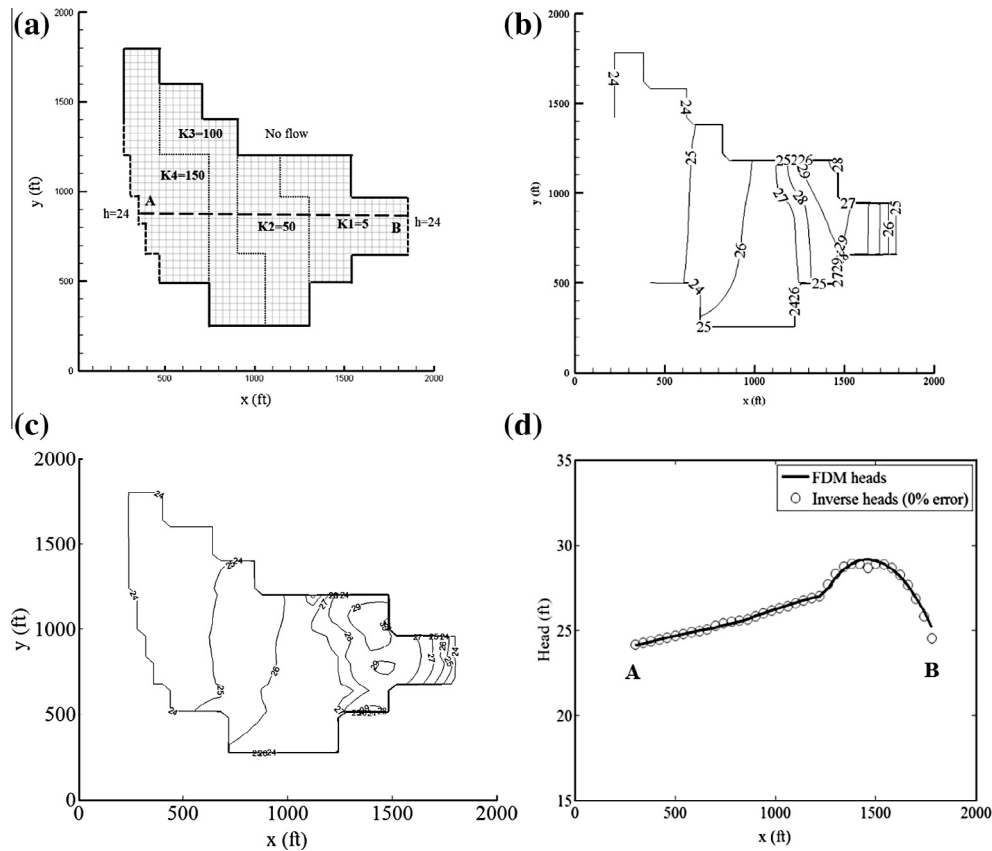


Fig. 9. (a) FDM true model of an unconfined aquifer with four conductivities ($K_1 = 5$, $K_2 = 50$, $K_3 = 100$, $K_4 = 150$) and $N = 0.01$. Location of a profile, AB, is shown at $y = 860$ ft. (b) Head contours predicted by the true model. (c) Head contours predicted by inversion when measurements are error-free. (d) Head profiles predicted along AB by the true model and by inversion.

Table 5

Inversion outcomes of an irregularly shaped unconfined aquifer, without and with pumping/injection wells. The estimated K and N parameters are in unit of ft/d.

	Hydraulic conductivities				Recharge	Number of inversion cells
	K_1	K_2	K_3	K_4	N	–
True parameters	5	50	100	150	0.01	–
Without pumping/injection 0% (0)	5.01	45.8	95.6	149.2	0.0091	31
With pumping/injection (0%)	5.1	48.9	101.7	148	0.0104	31
With pumping/injection ($\pm 0.25\%$)	5.3	49.3	107.2	149.3	0.0105	31

wells is added. Flux measurements are not needed. The same 31-cell grid is used in inversion. Results again yield accurate head recovery (Fig. 10c and d) and parameter estimation (Table 5).

3.2.3. Variable Recharge

With the same pumping and injection wells, the irregular-domain confined and unconfined problems with uniform recharge have been extended to problems where N is also heterogeneous, e.g., high recharge associated with hydrofacies with high conductivity, and vice versa. Similar inverse solutions are obtained whereas multiple K s, multiple N s, and the BC are estimated without the need for greatly increasing the number of measurements.

4. Discussion

By solving a set of problems with pumping and injection wells, we've demonstrated that subsurface flux measurements are not needed for the inverse method to succeed. Also, because pumping

rates can be easily measured at the surface, our method has low data requirement that is not much different from that used in interpreting classic pumping tests. For example, in using the Theim solution for parameter estimation, pumping rate in addition to aquifer heads is needed. Under non-pumping conditions, however, subsurface flux measurements are needed for the inversion to succeed. In aquifer model calibration, fluxes are not typically used by the existing inverse methods as a form of observation data [26]. However, it can be pointed out that the existing methods need to minimize an objective function (typically a model-data misfit), which requires the repeated simulations of the forward model. To do that, boundary conditions must be specified to this model, which usually include the Dirichlet-type BC (specified heads) and the Neumann-type BC (specified flux – a popular choice is the no-flux BC). (In transient calibration, initial conditions are also needed. This topic is not explored here.) Therefore, these methods in effect require that inversion be conditioned to a set of “flux measurements” along the Neumann boundary. In other words, by specifying a Neumann-type BC to a BVP in order to minimize an objective

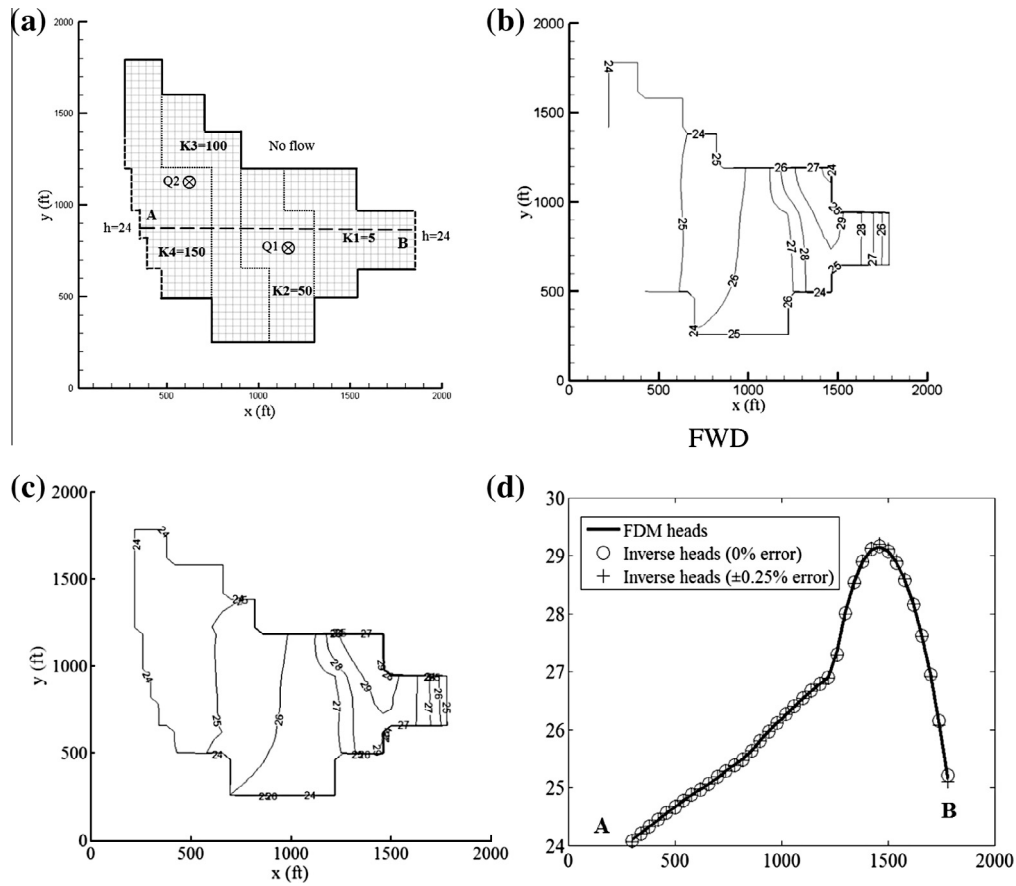


Fig. 10. Unconfined problem with a pair of pumping and injection wells: $Q1 = -500$ (pumping well) at (1100, 740) and $Q2 = 500$ (injection well) at (540, 1100). (a) FDM true model with four conductivities ($K1 = 5$, $K2 = 50$, $K3 = 100$, $K4 = 150$) and $N = 0.01$. Location of a profile, AB, is shown at $y = 860$ ft. In the forward model, to accurately compute the drawdowns, LGR (not shown) is performed at both well locations. (b) Head contours predicted by the true model. (c) Head contours predicted by inversion with 31 cells when measured heads contain $\pm 0.25\%$ errors. The same contour levels as those of the true model are used. (d) Head profiles predicted along AB by the true model and using inversion when measurement errors are increased.

function, the calibrated model by the existing methods in effect is “fitted” to these fluxes. The problem with this approach is that such fluxes are not real measurements that are sampled from the aquifer; rather they reflect a conceptual assumption made by the modeler. Because of subsurface uncertainty, if a wrong assumption of these BC is made (e.g., leakage exists along a presumed no-flux boundary), this will result in the so-called “model error” which is difficult to address using objective functions, e.g., various authors have discussed how the objective functions may be modified to account for “model errors” [37]. As demonstrated in Irsa and Zhang [9], because of the unknown BC, objective-function-based inversion can lead to non-uniqueness of both the estimated parameters and the flow fields. In the new method, the subsurface fluxes (or pumping rates) are provided to inversion at the locations where they are measured, which means that they can be anywhere inside the model domain or on the model boundaries. Compared to the objective-function-based approaches, no assumptions about the model BC are made, eliminating the possibility of making the type of “model errors” that can arise due to a wrong BC assumption.

Finally, with the new method (both in this study and in our earlier works), an issue exists with measuring subsurface groundwater fluxes or flow rates which are needed for inverting problems under non-pumping conditions. One way to address this is to conduct downhole flow logging under ambient flow [38]. Another approach can utilize hydrograph separation, although this technique requires that aquifer intersect streams whose gain/loss can be accurately measured to determine baseflows. In studying groundwater-surface water interactions, various seepage meters can be used to

directly measure water fluxes at the sediment interface [39]. Furthermore, an indirect approach can use Darcy’s Law to infer subsurface in situ fluxes based on local K measurements and hydraulic heads sampled in multilevel wells. For example, with the Multilevel Slug Test, a local K can be estimated at a packed-off interval [40]. If the same interval is subject to multiple head measurements under non-pumping conditions (i.e., at locations above and beneath this interval), an in situ groundwater flux can then be determined.

5. Conclusion

A two-dimensional physical-based inverse method is developed to simultaneously estimate multiple hydraulic conductivities, source/sink strengths, and boundary conditions, for both confined and unconfined aquifers. To address both non-pumping and pumping conditions, a unified theory is proposed by developing a set of hybrid fundamental solutions of inversion. Unlike the objective-function-based estimation techniques, this method does not require forward groundwater flow simulations to assess the model-data misfits, thus the knowledge of boundary conditions is not needed. It directly incorporates noisy observed data (hydraulic heads, groundwater fluxes, or well rates) at the measurement locations in a single step, without solving a boundary value problem. For both confined and unconfined aquifers, the method has been successfully tested on groundwater flow problems with regular and irregular geometries, different heterogeneity patterns, vari-

ances of heterogeneity, and measurement errors. Highlights of this study are summarized as follows:

1. Using nonlinear optimization, multiple hydraulic conductivities and recharge rates can be simultaneously inverted for 2D lateral flows in confined and unconfined aquifers that satisfy the Dupuit–Forchheimer assumption.
2. By employing the hybrid formulations, the inverse method can yield well-posed systems of equations that can be solved efficiently with coarse grids, with or without pumping wells. Solutions are also stable when measurement errors are increased, although the estimated parameters become less accurate.
3. Under non-pumping conditions, for both confined and unconfined problems, subsurface flux measurements are needed for inversion to succeed. When error-free observed data are used, the estimated conductivities and recharge rates are accurate within 8% of the true values (estimation errors can be further reduced with higher measurement density). Inversion is also accurate when aquifer conductivity has high contrast: the maximum successfully tested K_{max}/K_{min} of a confined aquifer problem is 10,000. The inversion outcomes are therefore insensitive to parameter variability.
4. The inverse method is able to handle model structure errors whereas the inverse formulation simplifies or complexifies the true parameter fields. For problems where the underlying parameter variation is unknown, equivalent conductivities and average recharge rates can be estimated. These parameters are physical-based, due to the fact that they're inferred from the conservation of mass and flux principles as enforced by the inverse method.
5. Under pumping conditions, flux measurements are not needed for the inversion to succeed. Therefore, data requirement of the inverse method is not much different from that of interpreting traditional well tests. With the hybrid formulation, local grid refinement near wells is not needed. Inversion can thus succeed with coarse grids, leading to high computation efficiency. Moreover, the inverse method can also handle problems where different types of boundary conditions as well as areal recharge can exert significant influences on the drawdowns at the wells.
6. Inversion accuracy is not sensitive to the degree of nonlinearity of the flow equation. Performance of the method for inverting confined and unconfined aquifer problems is similar in terms of the accuracy of the estimated parameters, the recovered head fields, and the solver speed.

The inverse method is based on superposing local analytical solutions of steady-state flow in a confined or unconfined aquifer subject to various source/sink effects. Caution is needed, however, when applying the method to real aquifers, where vertical flow can be significant near barriers such as impervious faults or engineered structures, or where borehole effects at the wells are non-negligible. Future work will investigate three-dimensional flow, extending the techniques of this study to problems with significant vertical flow. By imposing additional prior information equations that describe parameter structures (e.g., auto-covariance functions, cross-correlation with geophysical data, etc.), highly parameterized inversion will also be attempted.

Acknowledgment

This work is supported by the University of Wyoming Center for Fundamentals of Subsurface Flow of the School of Energy Resources (Grant ID: SER-CFSF-01-Zhang). The authors wish to thank the thoughtful comments of 3 anonymous reviewers.

References

- [1] Hantush MS, Jacob CE. Non-steady radial flow in an infinite leaky aquifer. *Trans. Am. Geophys. Union* 1955;36(1):95100.
- [2] Neuman S. Generalized scaling of permeabilities: validation and effect of support scale. *Geophys. Res. Lett.* 1994;21(5):349352.
- [3] Sanchez-Vila X, Carrera J, Girardi J. Scale effects in transmissivity. *J. Hydrol.* 1996;183:122.
- [4] Schulze-Makuch D, Carlson D, Cherkauer D, Malik P. Scale dependency of hydraulic conductivity in heterogeneous media. *Ground Water* 1999;37(6):904919.
- [5] Bouwer H, Rice RC. A slug test for determining hydraulic conductivity of unconfined aquifers with completely or partially penetrating wells. *Water Resour. Res.* 1976;12(3):423–8.
- [6] Zlotnik VA, Zurbuchen BR. Estimation of hydraulic conductivity from borehole flowmeter tests considering head losses. *J. Hydrol.* 2003;281:115–28.
- [7] Darnet M, Marquis G, Sallhac P. Estimating aquifer hydraulic properties from the inversion of surface Streaming Po-tential (SP) anomalies. *Geophys. Res. Lett.* 2003;30(13):1679. <http://dx.doi.org/10.1029/2003GL017631>.
- [8] Crisman SA, Molz FJ, Dunn DL, Sapping-ton FC. Application procedures for the electromagnetic borehole flowmeter in shallow unconfined aquifers. *Groundwater Monit. Rem.* 2007;12(3):96–100.
- [9] Irsa J, Zhang Y. A new direct method of parameter estimation for steady state flow in heterogeneous aquifers with unknown boundary conditions. *Water Resour. Res.* 2012;48:W09526. <http://dx.doi.org/10.1029/2011WR011756>.
- [10] Haitjema HM, Mitchell-Bruker S. Are water tables a subdued replica of the topography? *Ground Water* 2005;43(6):781–6.
- [11] Zhang Y, Gable CW, Person M. Equivalent hydraulic conductivity of an experimental stratigraphy – implications for basin-scale flow simulations. *Water Resour. Res.* 2006;42(7):W05404. <http://dx.doi.org/10.1029/2005WR004720>.
- [12] Zhang Y, Gable CW. Two-scale modeling of solute transport in an experimental stratigraphy. *J. Hydrol.* 2008;348:395–411. <http://dx.doi.org/10.1016/j.jhydrol.2007.10.017>.
- [13] Li W, Englert A, Cirpka OA, Vereecken H. Three dimensional geostatistical inversion of flowmeter and pumping test data. *Ground Water* 2008;46(2):193201.
- [14] Liu G, Chen Y, Zhang D. Investigation of flow and transport processes at the MADE site using ensemble Kalman filter. *Adv. Water Res.* 2008;31:975–86.
- [15] Cardiff M, Barrash W, Kitanidis PK, Malama B, Revil A, Straface S, Rizzo E. A potential-based inversion of unconfined steady-state hydraulic tomography. *Ground Water* 2009;47(2):259–70.
- [16] Simmers I. Groundwater recharge: an overview of estimation “problems” and recent developments. *Geological Society of London*; 1998. pp. 107–115.
- [17] Dettinger MD. Reconnaissance estimates of natural recharge to desert basins in Nevada, U.S.A., by using chloride balance calculations. *J. Hydrol.* 1989;106:55–78.
- [18] Scalon BR, Healy RW, Cook PG. Choosing appropriate techniques for quantifying groundwater recharge. *J. Hydrogeol.* 2002;10:1837.
- [19] Healy RW, Cook P. Using groundwater levels to estimate recharge. *Hydrogeol. J.* 2002;10(10):91109.
- [20] Tan S, Shuy E, Chua L. Regression method for estimating rainfall recharge at unconfined sandy aquifers with an equatorial climate. *Hydrol. Processes* 2007;21:35143526.
- [21] Lin YF, Wang J, Valocchi A. PRO-GRADE: GIS toolkits for ground water recharge and discharge estimation. *Ground Water* 2009;47(1):122–8. <http://dx.doi.org/10.1111/j.1745-6584.2008.00503.x>.
- [22] Pan L, Warrick AW, Wierenga P. Downward water flow through sloping layers in the vadose zone: time-dependence and effect of slope length. *J. Hydrol.* 1997;199:3652.
- [23] Russo D, Zaidel J, Lauter A. Numerical analysis of flow and transport in a combined heterogeneous vadose zone-groundwater system. *Adv. Water Res.* 2001;24:4962.
- [24] Jyrkama MI, Sykes JF, Norman SD. Recharge estimation for transient ground water modeling. *Ground Water* 2002;40(6):638–48.
- [25] Portniaguine O, Solomon D. Parameter estimation using groundwater age and head data, Cape Cod, Massachusetts. *Water Resour. Res.* 1998;34(4):637–45.
- [26] Hill MC, Tiedeman CR. *Effective groundwater model calibration: with analysis of data, sensitivities, predictions, and uncertainty*. 1st ed. Wiley-Interscience; 2007. p. 480.
- [27] Zhang Y. Nonlinear inversion of an unconfined aquifer: simultaneous estimation of heterogeneous hydraulic conductivities, recharge rates, and boundary conditions. *Transp. Porous Media* 2013, in press. <http://dx.doi.org/10.1007/s11242-014-0275-x>.
- [28] Butler Jr JJ, McElwee CD. Variable-rate pumping tests for radially symmetric nonuniform aquifer. *Water Resour. Res.* 1990;26(2):291–306.
- [29] Meier PM, Carrera J, Sanchez-Vila X. An evaluation of Jacob's method for the interpretation of pumping tests in heterogeneous formations. *Water Resour. Res.* 1998;34(5):1011–25.
- [30] Sanchez-Vila X, Meier PM, Carrera J. Pumping tests in heterogeneous aquifers: an analytical study of what can be obtained from their interpretation using Jacob's method. *Water Resour. Res.* 1999;35(4):943–52.
- [31] Yeh T-CJ, Liu S. Hydraulic tomography: development of a new aquifer test method. *Water Resour. Res.* 2000;36(8):2095–105.

- [32] Wu CM, Yeh T-CJ, Zhu J, Lee TH, Hsu N-S, Chen C-H, Sancho AF. Traditional analysis of aquifer tests: comparing apples to oranges? *Water Resour. Res.* 2005;41:W09402. <http://dx.doi.org/10.1029/2004WR003717>.
- [33] Firmani G, Fiori A, Bellin A. Three-dimensional numerical analysis of steady state pumping tests in heterogeneous confined aquifers. *Water Resour. Res.* 2006;42:W03422. <http://dx.doi.org/10.1029/2005WR004382>.
- [34] Tumlinson LG, Osiensky JL, Fairley JF. Numerical evaluation of pumping well transmissivity estimates in lateral heterogeneous formations. *Hydrogeol. J.* 2006;14:21–30.
- [35] Neumann SP, Blattstein A, Riva M, Tartakovsky DM, Gaudagnini A, Ptak T. Type curve interpretation of late-time pumping test data in randomly heterogeneous aquifers. *Water Resour. Res.* 2007;43:W10421. <http://dx.doi.org/10.1029/2007WR005871>.
- [36] D. Wang, Y. Zhang, J. Irsa, Dynamic data integration and stochastic inversion of a two-dimensional confined aquifer, in: *Proceedings, hydrology days, 2013*. <http://hydrologydays.colostate.edu/Papers_13/Dongdong_paper.pdf>.
- [37] Doherty J, Welter D. A short exploration of structural noise. *Water Resour. Res.* 2010;46:W05525. <http://dx.doi.org/10.1029/2009WR008377>.
- [38] Gelasch CA, Bradbury KR, Hart DJ, Bahr JM. Characterization of fracture connectivity in a siliciclastic bedrock aquifer near a public supply well (Wisconsin, USA). *Hydrogeol. J.* 2013;21:383–99.
- [39] Kalbus E, Reinstorf F, Schirmer M. Measuring methods for groundwater – surface water interactions: a review. *Hydrol. Earth Syst. Sci.* 2006;10:873–87.
- [40] Butler Jr JJ. Hydrogeological methods for estimation of spatial variations in hydraulic conductivity. In: Rubin Y, Hubbard SS, editors. *Hydrogeophysics*. Springer; 2005. p. 23–58.